ON SYNTHESIS OF CONTACT AIDED COMPLIANT MECHANISMS USING THE MATERIAL MASK OVERLAY METHOD*

Prabhat Kumar[†a], Roger A. Sauer[b], and Anupam Saxena[a]

[a]Mechanical Engineering , Indian Institute of Technology Kanpur, 208016, India , kprabhat@iitk.ac.in
[b]Mechanical Engineering , AICES, RWTH Aachen University, Templergraben 55, 52056 Aachen, Germany, sauer@aices.rwth-aachen.de
[a]Mechanical Engineering , Indian Institute of Technology Kanpur, 208016, India , anupams@iitk.ac.in

Published[1] in *ASME 2015 International Design Engineering Technical Conferences and Computers and Information in Engineering Conference IDETC/CIE 2015 August 2-5, 2015, Boston, Massachusetts, USA*
DOI: 10.1115/DETC2015-47064
Submitted on 26. January 2015, Accepted on 16. March 2015, Final manuscript submitted on 20. April 2015

Abstract Contact Aided Compliant Mechanisms (CCMs) are synthesized via the Material Mask Overlay Strategy (MMOS) to trace a desired non-smooth path. MMOS employs hexagonal cells to discretize the design region and engages negative circular masks to designate material states. To synthesize CCMs, the modified MMOS presented herein involves systematic mutation of five mask parameters through a hill climber search to evolve not only the continuum topology (slave surfaces), but also, to introduce the desired rigid, interacting surfaces within some masks. Various geometric singularities are subdued via hexagonal cells though numerous V-notches get retained at the continuum boundaries. To facilitate contact analysis, boundary smoothing is performed by shifting boundary nodes of the evolving continuum systematically. Numerous hexagonal cells get morphed into concave sub-regions as a consequence. Large deformation finite element formulation with Mean Value Coordinates (MVC) based shape functions is used to cater to the generic hexagonal shapes. Contact analysis is accomplished via the Newton-Raphson iterations with load increment in conjunction with the penalty method and active set constraints. An objective function based on Fourier Shape Descriptors is minimized subject to suitable design constraints. An example of a path generating CCM is included to establish the efficacy of the proposed synthesis method.
Keywords: Contact-aided compliant mechanisms; MMOS; topology optimization; Boundary smoothing, Fourier Shape Descriptors;

*Honorable Mention Fast Forward Presentation Award
†Corresponding author, email: kprabhat@iitk.ac.in

1 Introduction

1.1 Compliant Mechanisms

Compliant mechanisms (CMs) transfer input loads to a desired output by virtue of their monolithic composition. Two well-established methods exist to synthesize CMs, (a) the Pseudo Rigid Body Model approach and (b) the continuum optimization approach. Among the many existing topology optimization approaches, the Homogenization method by Kikuchi and Bendsøe [1] aimed at determining the optimal size of an elliptic void within a solid cell. An array of such cells comprised the stiffest possible structure under a resource constraint. Ananthasuresh [2] extended the Homogenization approach to synthesize compliant mechanisms systematically. Ananthasuresh et al. [3] maximized the desired output displacement in addition to maximizing stiffness of the mechanism. Frecker et al. [4] and Nishiwaki et al. [5] used ratio of the two objectives and reported improvement in convergence. Using the SIMP (Solid Isotropic Method with Penalization) method [6–8], Sigmund [9] proposed to maximize the mechanical advantage (ratio of the output force F_{out} to the input load F_{in}) with suitable constraints on input displacements and volume. In SIMP, cell density (ρ_i) is considered as a design variable. $\rho_i = \epsilon > 0$ models void cells while $\rho_i = 1$ models cells with the desired material. A small positive ϵ is chosen to circumvent singularity in the stiffness matrix during the finite element analysis. Elastic modulus of a cell is modeled as $E_i = E_0\rho_i^n$, where $n(\geq 3)$ is a penalty parameter that helps accelerate the optimization algorithm to converge towards a binary solution. E_0 is the modulus of the desired material. To design compliant mechanisms, other material models similar to SIMP were based on the normal distribution (the PEAK model [10]) and logistic functions (the SIGMOID model [11]).

Most aforementioned methods employed rectangular shaped cells to analyze the evolving continuum via the finite element analysis. These discretization schemes suffer from geometric singularities like the checkerboard patterns, point flexures and islanding [12] to circumvent which, additional suppression, filtering or penalty based methods are required [13, 14] [15, 16] [11, 17–20]. Rahamatalla and Swan [12] proposed a two stage optimization formulation by introducing artificial springs, one at the input location and other at the output position. They suggested to increase the stiffness of springs attached to the output port to obtain compliant mechanisms free from point flexures.

Numerous similar approaches in topology optimization have used discrete (truss, and/or frame elements) or continuum (rectangular, hexagonal or polygonal cells) parameterization and have optimized various measures of flexibility and stiffness (generalized in [21]) to synthesize monolithic compliant mechanisms under the small deformation assumption.

Path generating compliant mechanisms undergo large deflections to trace a specified path. Saxena and Ananthasuresh [22] and Pedersen et al. [23] considered geometric nonlinearity in their synthesis methods. Objectives based on least square discrepancies [22–24] were employed to minimize the variation in the specified and actual paths. The least square objective fails to compare the shape, size and orientation of the two path individually. Ullah and Kota [25] employed Fourier shape descriptors [26] to help a designer exercise individual control over the shape, size and orientation of paths. Rai et. al [27, 28] demonstrated that large, nonlinear and nonsmooth paths can be traced by an assemblage of deformable curved and rigid linear members to synthesize path generating fully and partially compliant mechanisms respectively. The latter, even though capable of tracing a desired non-smooth path, were bulky and required significant effort and care when assembling different components.

1.2 Contact-Aided Compliant Mechanisms

The notion of contact based deformation was first proposed and exploited by Mankame and Ananthasuresh [29, 30] to achieve non-smooth paths in particular via monolithic compliant mechanisms. Mankame and Ananthasuresh termed such continua as Contact-Aided Compliant Mechanisms or CCMs. Besides path generation, interesting deformation characteristics like negative stiffness, static balancing and others can be achieved through CCMs. For their topology synthesis, linear [24, 29, 30] and curved frame elements [27, 31] were employed for design parameterization and geometrically nonlinear finite element analysis. In [30], intermittent but prespecified contact surfaces were used. Reddy et. al. [31] synthesized monolithic, path generating CCMs by modeling the design region with discrete curved members. Contact surfaces were not prespecified, rather determined systematically.

2 Motivation and Organization

We demonstrate topology synthesis of path generating contact-aided compliant mechanisms via continuum elements. Such an approach has not been proposed yet. We employ hexagonal cells for domain representation and negative circular masks to not only help identify the continuum topology, but also, to render rigid contact surfaces in the neighborhood so that the continuum can interact physically with such surfaces.
The paper is organized as follows. In section 3, the Material Mask Overlay Method is discussed briefly followed by its modified version (CMMOS) to synthesize CCMs. Sections 4 and 5 outline boundary smoothing, large deformation finite element analysis with contact and formulation of the path generating objective. The hill climber search algorithm is also discussed. Results are presented thereafter and conclusions are drawn.

3 Material Masks Overlay Strategy (MMOS)

The Material Mask Overlay Method (MMOS) [19, 32–34] uses hexagonal cells (Ω_{H}) for domain (Ω) discretization and engages negative circular masks (Ω_{M}) to designate the material state $\rho(\Omega_H)$ to each cell within the domain. Through hexagonal tessellation, *edge-connectivity* is ensured throughout the domain thereby guaranteeing finite stiffness everywhere within the design region. Each Ω_{M} is associated with three variables $(x_i,\ y_i,\ r_i)$, where $(x_i,\ y_i)$ are the center coordinates of the mask and r_i is its radius. All cells with centroids inside any mask are modeled *void*. The continuum is thus defined by the set of remnant cells that are not exposed to any mask. That is, the centroids of such *filled* cells do not lie within any negative mask. Mathematically, the material state of a cell is described as

$$\rho(\Omega_{\mathrm{H}}) = \begin{cases} 0, & \text{if } \Omega_{\mathrm{H}}^{\mathrm{c}} \subset \text{ any } \Omega_{\mathrm{M}}\ (d_{\mathrm{cm}} - r_{\mathrm{m}} \leq 0) \\ 1, & \text{if } \Omega_{\mathrm{H}}^{\mathrm{c}} \not\subset \text{ any } \Omega_{\mathrm{M}}\ (d_{\mathrm{cm}} - r_{\mathrm{m}} > 0) \end{cases} \tag{1}$$

where d_{cm} is the distance between the centroid of the hexagonal cell and the mask, and $\Omega_{\mathrm{H}}^{\mathrm{c}}$ represents the centroid of Ω_{H} (Fig. 1a). Following generic topology optimization problem can be solved to get the desired continuum.

$$\begin{aligned} \underset{\mathbf{v}}{\text{minimize}} \quad & f_0(\mathbf{v}) \\ \text{subject to} \quad & g_j(\mathbf{v}) \leq 0 \end{aligned} \tag{2}$$

$f_0(\mathbf{v})$ is the desired objective and $g_j(\mathbf{v}) \leq 0$ are the imposed design constraints. $\mathbf{v}$, the design vector, comprises of a set of variables $\{(x_m,\ y_m,\ r_m)\}\ \forall\ \ \Omega_{\mathrm{M}}$.

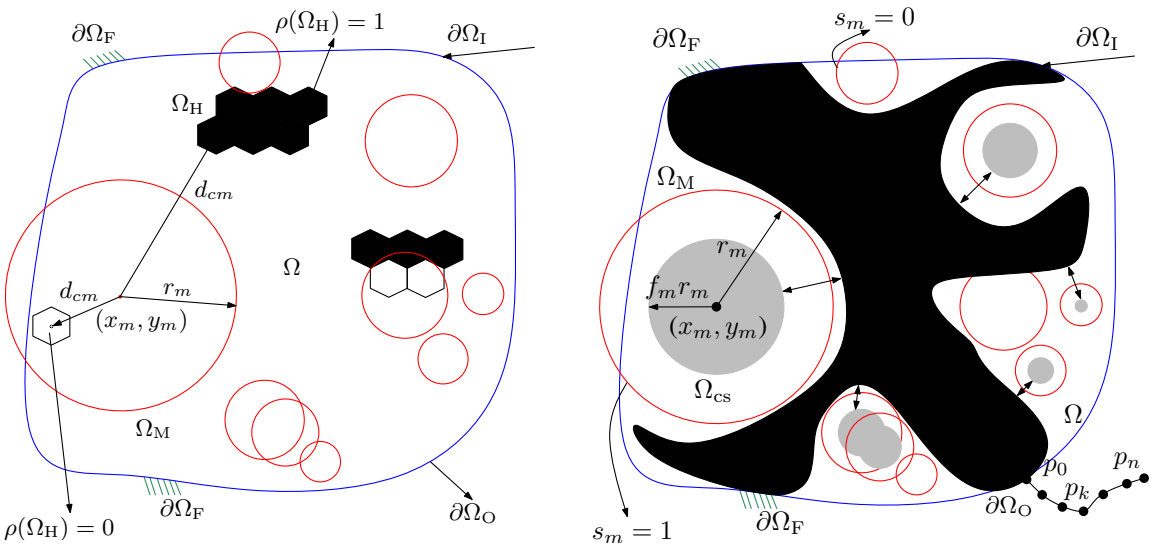

Figure 1: Hexagonal cells Ω_{H} are used to discretize the design domain Ω shown with superposed negative circular masks Ω_{M}. Masks are engaged to remove the material beneath them and also, to generate rigid contact surfaces. They are characterized via five parameters (x_m, y_m, r_m, s_m, f_m). $s_{\mathrm{m}} = 1$ indicates that the m^{th} mask generates a contact surface within it while with $s_{\mathrm{m}} = 0$ only the material is removed. $\rho(\Omega_{\mathrm{H}}) = 0$ (cells whose centroids are inside a mask) implies that the hexagonal sub-region has no material while $\rho(\Omega_{\mathrm{H}}) = 1$ (cells whose centroids are outside the mask) suggests that the cell has the desired material. Boundary(ies) of the continuum generated via $\rho(\Omega_{\mathrm{H}}) = 1$ is (are) smoothened. Masks with $s_{\mathrm{m}} = 1$ interact with the continuum to render the desired path. Fixed boundary(ies) of the domain, input and output conditions are depicted.

3.1 Contact MMOS

The goal herein is to synthesize contact-aided compliant mechanisms (CCMs) via the material mask overlay method (MMOS). The concept is extended such that masks not only remove material beneath them, but also, within some, fixed, non-deforming regions [2] are introduced to permit the continuum to physically interact with them. To accomplish this, each mask Ω_{Mi} is represented via five variables: (x_i, y_i, r_i, s_i, f_i). The first three represent the x, y coordinates of the mask center and mask radius respectively. The fourth variable s_i is discrete; $s_i = 0$ indicates absence of the contact surface Ω_{cs} within itself while $s_i = 1$ models the presence of a circular contact region whose radius is computed as $f_i r_i, 0 \leq f_i < 1$ with its center coordinates the same as (x_i, y_i). Fig. 1b depicts the overall notion. Although a single mask can introduce a contact surface which is circular in shape, a set of such overlapping masks (permitted within the proposed framework) can yield a contact region of any shape at the desired location. Contact interaction is permitted only between the continuum and rigid regions introduced by the masks. It is assumed that neighboring regions of the continuum itself do not interact.

[2] Contact surface Ω_{CS}

4 Boundary smoothing and Finite Element Analysis

4.1 Boundary smoothing

Hexagonal cells do help eliminate geometric singularities, however, boundaries of the final continuum are serrated containing numerous V-notches. Boundaries with only C^0 continuity, as is the case with hexagonal tessellation[3], pose severe difficulties in contact analysis. In addition, pointed notches are also regions of stress concentration. To ensure convergence in contact analysis, continuum boundaries (interior and exterior) should at least have slope (C^1) continuity though higher order continuity is desirable. A systematic approach to boundary smoothing requires the mid-points of the outer edges of the boundary cells to be connected with straight line segments, and boundary nodes to be projected onto these segments along their shortest perpendiculars (Fig. 2a). This smoothing step can be performed $\beta > 1$ times. New positions of the boundary nodes are used in the finite element analysis, while retaining the element connectivity and positions of the interior (non-boundary) nodes. Details of the implemented boundary smoothing approach are provided in [20].

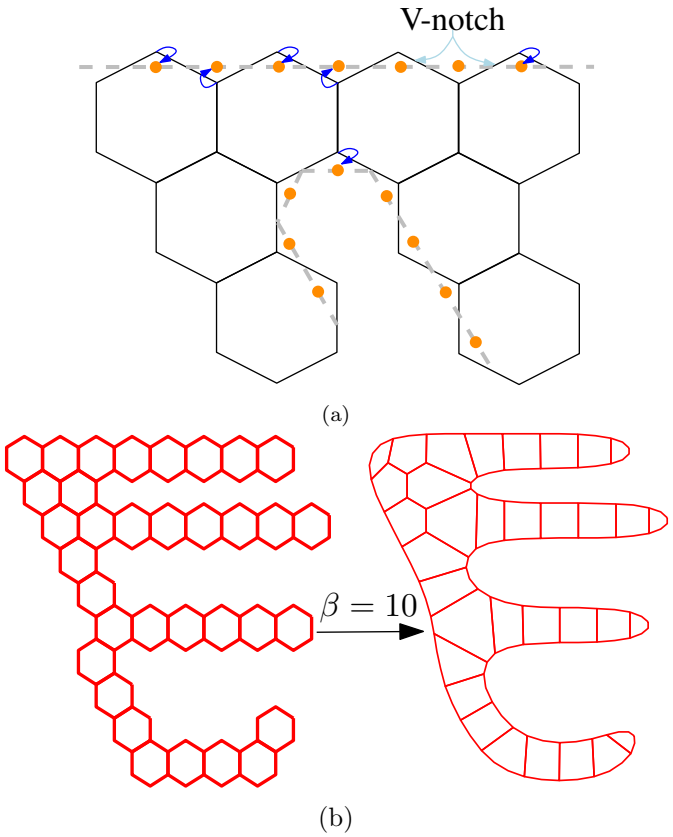

Figure 2: Many V-notches get retained on the continuum boundaries. (a) Mid-points of boundary edges are joined with straight lines and boundary nodes shifted along their shortest perpendicular distance on these segments. (b) (left) no boundary smoothing and (right) smoothing with $\beta = 10$ steps.

4.2 Stiffness Computation

As a result of boundary smoothing, some regular hexagonal cells get reshaped to concave ones. To cater to both shapes, Mean-Value Co-ordinates [35–37] based shape functions are employed.

[3] other discretization schemes also suffer from the same anomaly

Stiffness $\boldsymbol{k}$ of each cell is evaluated as follows. The cell is divided into six triangular sub-regions [38]. Thereafter, integration over each region is performed through a 25 Gauss-points scheme for each sub-region (Fig. 3a). Geometrically nonlinear analysis with Newton-Raphson (NR) iterations for a sequence of load increments is implemented. Within each NR iteration, contact forces between the deforming continuum and rigid bodies need to be computed which is accomplished in the following section.

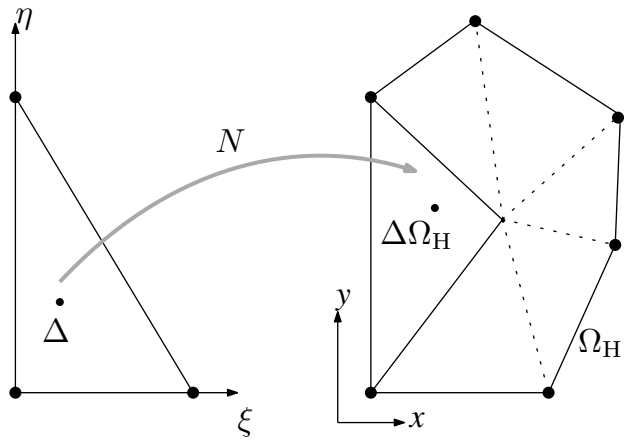

(a)

Figure 3: Each cell is divided into six subregions and integration over each subpart is performed to evaluate the element stiffness matrix $\boldsymbol{k}$.

5 Contact Modeling and Analysis

Let a rigid body Ω_{cs} (contact surface) come in contact with a part of the deforming body Ω_s (optimal continuum) (Fig. 4). Let points P_m on Ω_{cs} and P_s on Ω_s have position vectors $\mathbf{x}_m$ and $\mathbf{x}_s$ respectively. Let the normal triad at P_s be $\mathbf{n}^s_a$, $a = 1, 2, 3$ and that at P_m be $\mathbf{n}^m_b$, $b = 1, 2, 3$. Consider $\mathbf{n}^c_1$, $c = m, s$ to be outward normals and remaining to be tangential components at P_m and P_s respectively. Let the tractions at P_s and P_m be $\mathbf{t}_s$ and $\mathbf{t}_m$ ($\mathbf{t}_s = -\mathbf{t}_m$) respectively. The gap between these surfaces is defined as

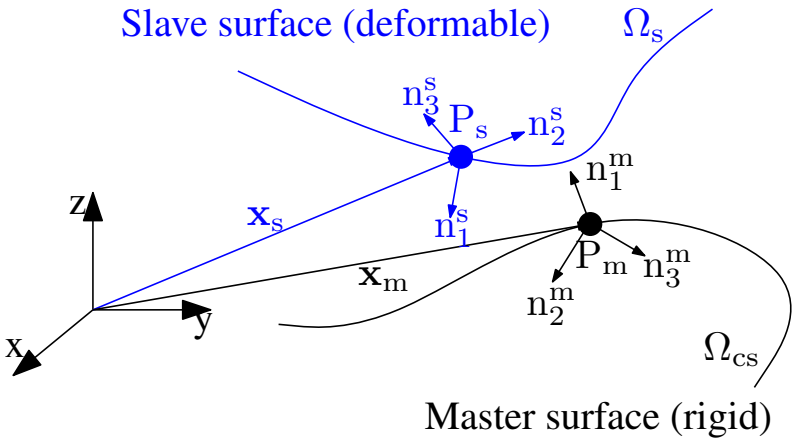

Figure 4: Contact formulation between two bodies Ω_s and Ω_{cs}. Normal triad on P_s are n^s_i and that on P_m are n^m_i, where $i = 1, 2, 3$.

$$\mathbf{g} = \mathbf{x}_\mathrm{s} - \mathbf{x}_\mathrm{m} \tag{3}$$

The normal gap $\mathbf{g}_\mathrm{n}$ can be defined via either $(\mathbf{x}_\mathrm{s} - \mathbf{x}_\mathrm{m}).\mathbf{n}_1^\mathrm{s}$ or $(\mathbf{x}_\mathrm{m} - \mathbf{x}_\mathrm{s}).\mathbf{n}_1^\mathrm{m}$. When Ω_cs and Ω_s are in contact, $\mathbf{g}_\mathrm{n}$ equals zero. The following impenetrability condition is then invoked.

$$\begin{aligned}(\mathbf{x}_\mathrm{s} - \mathbf{x}_\mathrm{m}).\mathbf{n}_1^\mathrm{s} = 0\\ (\mathbf{x}_\mathrm{m} - \mathbf{x}_\mathrm{s}).\mathbf{n}_1^\mathrm{m} = 0\end{aligned} \tag{4}$$

When in contact, traction components along the outward normals $\mathbf{n}_1^\mathrm{c}$ are compressive (< 0), otherwise they are zero.

$$\mathrm{t}_1^\mathrm{c} = \mathbf{t}^\mathrm{c}.\mathbf{n}_1^\mathrm{c} \leq 0; \quad \mathrm{c} = \mathrm{m}, \mathrm{s} \tag{5}$$

To check for slipping/sliding

$$\mathrm{t}_2^\mathrm{c} = \mathbf{t}^\mathrm{c}.\mathbf{n}_2^\mathrm{c} \text{ and } \mathrm{t}_3^\mathrm{c} = \mathbf{t}^\mathrm{c}.\mathbf{n}_3^\mathrm{c}; \quad \mathrm{c} = \mathrm{m}, \mathrm{s} \tag{6}$$

are used. $(t_2^c \cdot t_2^c + t_3^c \cdot t_3^c)^{\frac{1}{2}} < \mu(t_1^c t_1^c)$ for stiction, else for sliding, equality sign should be used. To model contact problems herein, impact is assumed to be absent. In addition to contact conditions, relations for equilibrium, strain displacement, constitutive and boundary restraints can be written mathematically as

$$\sigma_{ij,j}(\mathbf{x}) + b_i(\mathbf{x}) = 0, \mathbf{x} \in \Omega_\mathrm{cs}, \Omega_\mathrm{s} \tag{7}$$
$$\epsilon_{ij}(\mathbf{x}) = 0.5(u_{i,j} + u_{j,i} + u_{k,i}u_{k,j}) \tag{8}$$
$$S_{ij}(\mathbf{x}) = E_{ijkl}\epsilon_{kl}(\mathbf{x}) \tag{9}$$
$$\mathbf{u}(\Gamma_{dc}) = \mathbf{u}_c, \ c = m, s; \tag{10}$$
$$\sigma_{ij}(\Gamma_{Fc})n_j(\Gamma_{Fc}) = f_i(\Gamma_{Fc}) \tag{11}$$

σ_{ij} and ϵ_{ij} represent the Cauchy stress and strain tensor components respectively. b_i is the body force, S_{ij} is the second Piola-Kirchoff stress tensor, E_{ijkl} is the elastic tensor, Γ_{dc} represent boundaries on two surfaces, where displacements $\boldsymbol{u}_c$ is known a priori, and tractions f_i are imposed on surfaces Γ_{Fc} of the two bodies. The transformation, $\boldsymbol{S} = \det(\boldsymbol{F})\boldsymbol{F}^{-1}.\boldsymbol{\sigma}.\boldsymbol{F}^{-T}$ is employed to relate Cauchy stress and second Piola-Kirchoff stress tensors.

6 Problem formulation

6.1 Objective evaluation

We demonstrate the synthesis of CCMs of which the prescribed output point traces a given large, non-smooth path. Fourier Shape Descriptors (FSDs) [25–27,30,31] are employed to evaluate the objective which is modeled to capture discrepancies in the global shape, size, and orientation between the actual and desired paths. To have a control over the resource volume of the final continuum, $(V^c - V^*)$ is introduced in the FSDs objective, where V^c and V^* are the current volume and permitted volume respectively. Let the Fourier coefficients of the actual path traced by the candidate design be a_α and b_α and that of the desired path be a_δ and b_δ. Let the length of the desired path be L_δ and that of the actual path be L_α. Let the initial orientations with the horizontal, of the two paths be given by θ_δ and θ_α respectively. The objective is constructed as the weighted sum of the errors in each coefficient, length and orientation, as below.

$$f_0(\mathbf{v}) = \lambda_a a_{err} + \lambda_b b_{err} + \lambda_L L_{err} + \lambda_\theta \theta_{err} + \lambda_v (V^c - V^*) \tag{12}$$

where $\lambda_a, \lambda_b, \lambda_L,\ \lambda_\theta$ and λ_v are user defined weights. The first four weights control the contribution of each error term and the last one governs the resource volume of the continuum. These errors are given by

$$\begin{aligned} a_{err} &= \sum_{f=1}^{N} (a_\delta - a_\alpha)^2 \\ b_{err} &= \sum_{f=1}^{N} (b_\delta - b_\alpha)^2 \\ L_{err} &= (L_\delta - L_\alpha)^2 \\ \theta_{err} &= (\theta_\delta - \theta_\alpha)^2 \end{aligned} \tag{13}$$

6.2 Search Algorithm

To minimize the objective, we employ a random mutation based stochastic, hill climber search. An initial solution $\mathbf{v}_0$ is taken and made to undergo several mutations to sequentially improve the objective. Maximum number of iterations I_{mmos} is fixed a priori. For N_{m} masks, the total number of variables in $\mathbf{v}_0$ are $5N_{\text{m}}$. Let the probability to mutate a variable $d \in \mathbf{v}_0$ be pr, (chosen 0.08 herein). In an iteration, a random number ζ is generated for each variable. If $\zeta < pr$, the corresponding variable is modified as $d_{\text{n}} = d \pm (c \times m_{\max})$. Where c is a random number and $m_{\max}$ is used as 25% of the domain size. Variables $x_i, y_i, r_i,\ f_i$ and s_i of a mask are mutated as above. As s_i is binary, an additional check is performed. If $s_i < 0.5$, $s_i = 0$ is imposed, else, $s_i = 1$ is taken. The aforementioned mutations lead to a new design $\mathbf{v}_n$ which is evaluated using the finite element analysis and Fourier Shape Descriptors. If found better, $\mathbf{v}_0$ is replaced by $\mathbf{v}_n$. The search process is continued until I_{mmos} iterations are reached. Cardinal reasons to employ stochastic search are: (a) Cell densities should either be 0 or 1 for otherwise ambiguity in interpreting the continuum may lead to incomplete/poor realization of the solution, and (b) non-convergence during Newton-Raphson iterations in the finite element analysis can stall a gradient search process as the latter is based on point-to-point stepsize evaluation. For subsequent advancement to the next step of search, convergence in analysis in the previous step is necessary. For any intermediate continuum, accomplishment of geometrically nonlinear analysis, and with contact in particular, cannot be guaranteed.

7 Synthesis Example

The proposed method is applied to an example problem. Figure 6 depicts the design specifications and Table 1 includes values of various parameters used (Fig. 6):

The design region is represented using 25 hexagonal cells along the horizontal direction and 25 cells along the vertical direction. Negative masks are initialized with 8 masks along the horizontal and the same number along the vertical. Minimum and maximum mask radii are taken as 0.1 mm and 6 mm respectively. Out of plane thickness is 1 mm, Elastic modulus is 2000 MPa, and Poisson's ratio is 0.29. For the hill climber search, probability that a variable can mutate is taken as 0.08. Maximum number of search iterations I_{mmos} are set to 40, 000. Input load is also considered a design variable whose lower and upper bounds are set to -1000 N and 1000 N. Note that direction of the input load is permitted to change. Maximum radius achievable for the contact surface is 4.5 mm (i.e., $f_i(\max) = 0.9$).

Number of boundary smoothing steps performed for each candidate continuum is 10. Among other parameters, weights of the Fourier Shape Descriptors are set to $\lambda_{\text{a}} = 18$ and $\lambda_{\text{b}} = 18$. Weight for discrepancy in the length is taken as $\lambda_{\text{L}} = 0.18$ while that for the orientation is

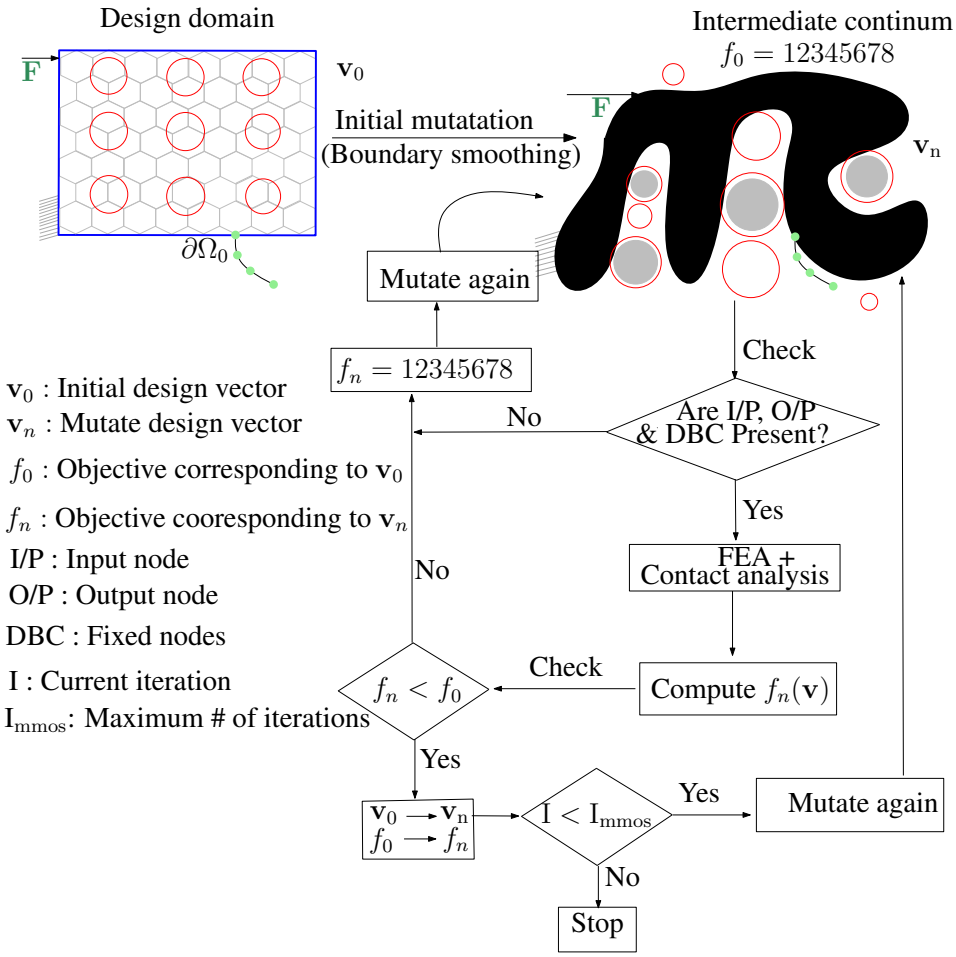

Figure 5: Ω is discretized via hexagonal cells Ω_{H}. Negative circular masks Ω_{M} are employed to remove the material and to yield contact surfaces within some. Contact analysis with minimization of the Fourier Shape Descriptors based objective is performed to achieve the path close to that desired.

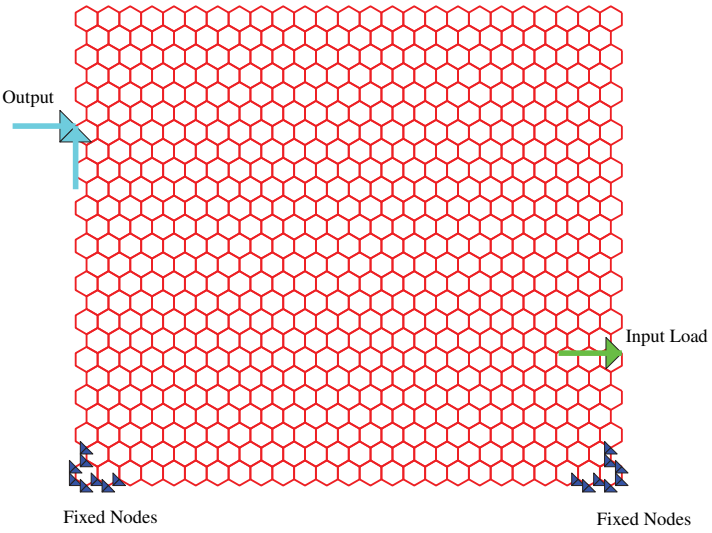

Figure 6: The design space is represented via hexagonal cells. Input load, output port and boundary condition are also shown

.

$\lambda_\theta = 0.01$. The desired path is the inverted V shape shown on the left corner in Figs. 7 and 9 which also show the undeformed optimized continuum in red and the final deformed continuum

Parameter's name	**Units**	**Value**
Design domain	$\cdots$	$25HCH \times 25HCV$
# of Ω_{M} in horizontal direction (N_{x})	$\cdots$	8
# of Ω_{M} in vertical direction (N_{y})	$\cdots$	8
Maximum radius of Ω_{M}	mm	6.0
Minimum radius of Ω_{M}	mm	0.1
Maximum # of iterations	$\cdots$	40000
Out of plane thickness	mm	1.0
Young's modulus	MPa	2000
Poisson's ratio	$\cdots$	0.29
Permitted volume fraction ($\frac{V^*}{V}$)	$\cdots$	0.30
Mutation probability	$\cdots$	0.08
Contact surface radii factor	$\cdots$	0.90
Maximum mutation size ($m_{\max}$)	$\cdots$	6
Upper limit of the load (UPP$\boldsymbol{F}$)	N	1000
Lower limit of the load (Low$\boldsymbol{F}$)	N	-1000
Weight of a_{err} (λ_{a})	$\cdots$	18
Weight of b_{err} (λ_{b})	$\cdots$	18
Weight of path length error (λ_{L})	$\cdots$	0.18
Weight of path orientation error (λ_θ)	$\cdots$	0.01
Boundary smoothing steps (β)	$\cdots$	10

Table 1: Parameters used in the synthesis for the example 1. Herein, HCH represents the number of hexagonal cells in the horizontal direction and HCV indicates the number of hexagonal cells in the vertical direction.

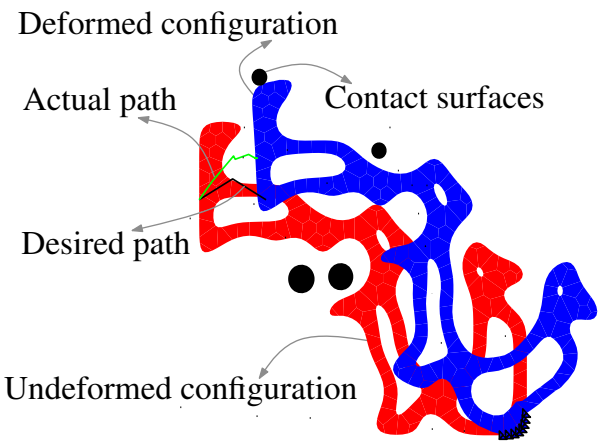

Figure 7: Undeformed (red solid), deformed (blue solid), contact surfaces (black solid), the desired path (black straight line) and the actual path (green straight line) are shown.

in blue. Herein, two solutions (Figs. 7 and 9) are depicted for the same problem, emphasizing that multiple solutions can exist. One can notice that there are many kinks present in the obtained path. Reason for their presence is that boundaries of both, the continuum and contact surface(s) are modeled as piece-wise linear. Such kinks can be subdued if interacting boundaries are modeled as splines, e.g., by incorporating isogeometric analysis for contact. The circles in black are the contact surfaces suggested by the algorithm. The actual path is shown in green. As the continuum deforms, it engages with the contact surface. Few kinks are observed at the trailing end of the actual path. One notices that many contact surfaces do not participate in deformation and hence can be ignored. A resource constraint is employed via a penalty term,

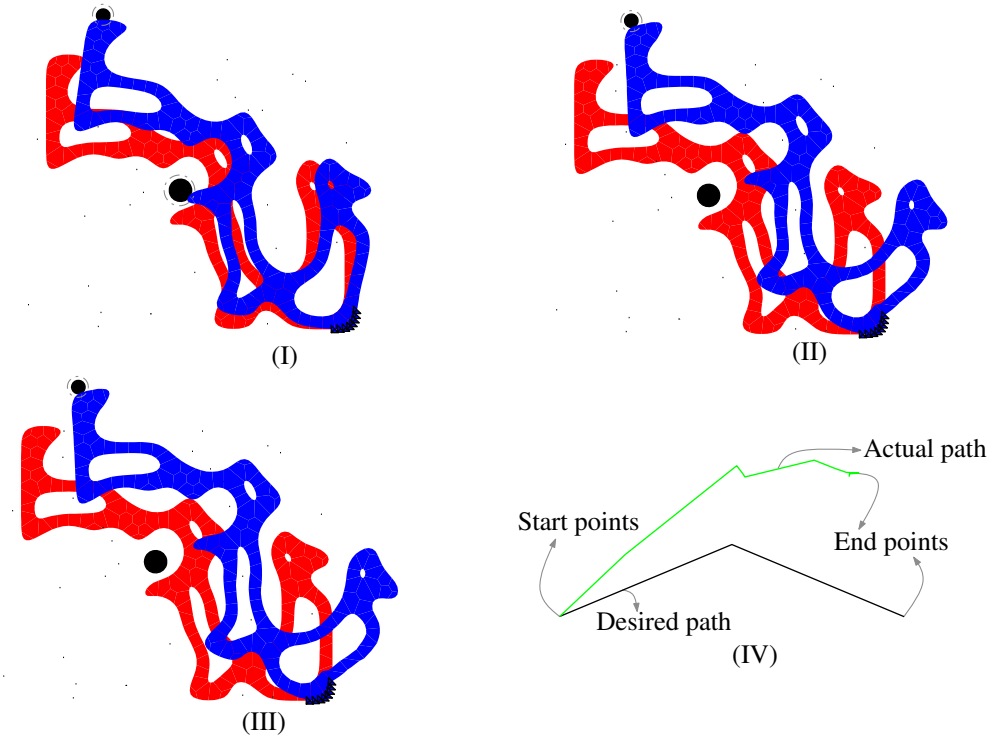

Figure 8: Different deformed configurations are shown in (I,II,III). (IV) shows comparison of the desired and actual paths.

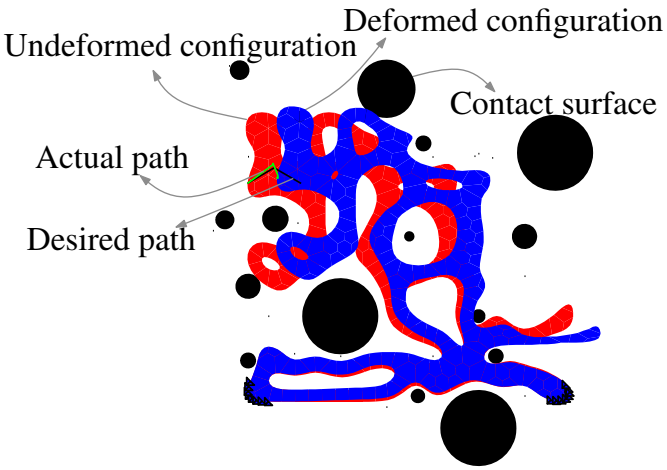

Figure 9: Undeformed (red solid), deformed (blue solid), contact surfaces (black solid), the desired path (black straight line) and the actual path (green straight line) are shown.

$\lambda_v(V^c - V^*)$ in Eq. (12). V^* is taken as 30% of the maximum possible volume V. λ_v is taken as 15 if the continuum volume V^c exceeds V^*, else, λ_v is set to 0. In addition to removing hexagonal cells beneath the masks, regular hexagonal cells (e.g., those that are unaffected by boundary smoothing) are removed. This is equivalent to imposing negative masks such a cell. In addition, such removal also helps reduce the continuum volume making the latter less bulky and members slender so that they can undergo large local deformation.

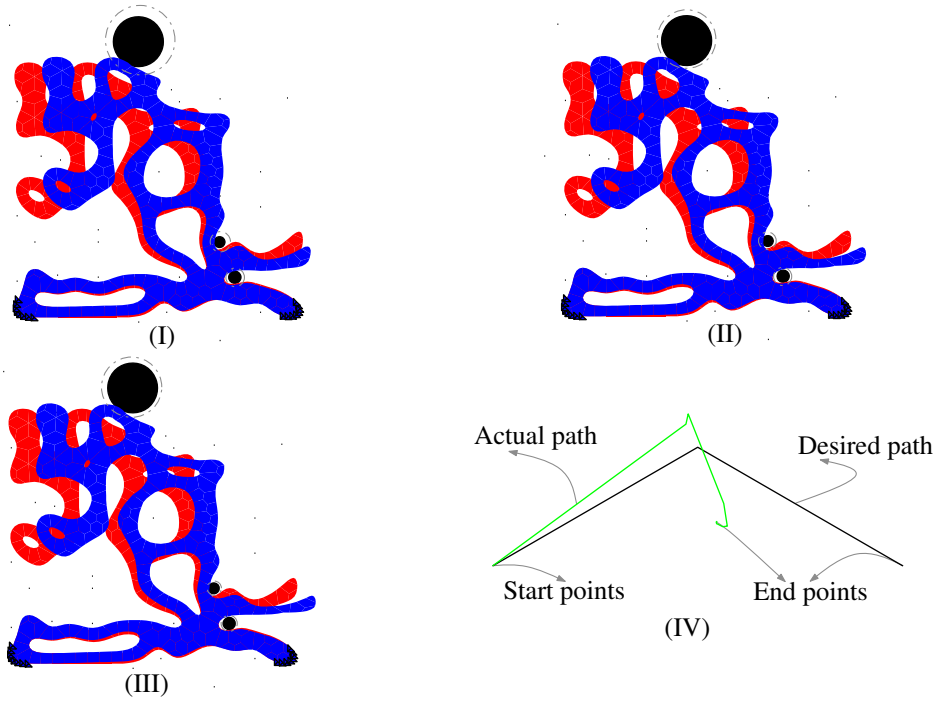

Figure 10: Different deformed configurations are shown in (I,II,III). (IV) shows comparison of the desired and actual paths.

8 Conclusion

We present a continuum based topology optimization approach for the first time to synthesize monolithic contact-aided compliant mechanisms via the modified Material Mask Overlay Method (CMMOS). Hexagonal cells are used to discretize the design space. Negative masks are not only employed to remove material, but also, to generate rigid contact surfaces within some of them. Boundary smoothing is implemented to facilitate contact analysis. Mean-Value Coordinates based shape functions are used to cater to both, convex and concave shaped cells. A stochastic hill climber search is implemented to minimize the Fourier Shape Descriptors based objective to obtain the desired non-smooth path. Preliminary results are promising in that the proposed continuum optimization method can be employed to synthesize, not only contact-aided compliant mechanisms, but also, those with, say static balancing and negative stiffness characteristics. Detailed investigations on and synthesis of more examples with the proposed synthesis method are planned in future.

9 Acknowledgment

The first and third authors acknowledge Shyam Sunder Nishad for his help in preparation of this manuscript.

References

[1] M. P. Bendsøe and N. Kikuchi, "Generating optimal topologies in structural design using a homogenization method," *Computer methods in applied mechanics and engineering*, vol. 71, no. 2, pp. 197–224, 1988.

[2] G. Ananthasuresh, S. Kota, and Y. Gianchandani, "A methodical approach to the design of compliant micromechanisms," in *Solid-state sensor and actuator workshop*, vol. 1994, pp. 189–192, SC: IEEE, 1994.

[3] G. Ananthasuresh, S. Kota, and N. Kikuchi, "Strategies for systematic synthesis of compliant mems," in *Proceedings of the 1994 ASME winter annual meeting*, pp. 677–686, 1994.

[4] M. Frecker, G. Ananthasuresh, S. Nishiwaki, N. Kikuchi, and S. Kota, "Topological synthesis of compliant mechanisms using multi-criteria optimization," *Journal of Mechanical design*, vol. 119, no. 2, pp. 238–245, 1997.

[5] S. Nishiwaki, M. I. Frecker, S. Min, and N. Kikuchi, "Topology optimization of compliant mechanisms using the homogenization method," 1998.

[6] G. Rozvany, M. Zhou, and T. Birker, "Generalized shape optimization without homogenization," *Structural Optimization*, vol. 4, no. 3-4, pp. 250–252, 1992.

[7] M. P. Bendsøe, "Optimal shape design as a material distribution problem," *Structural optimization*, vol. 1, no. 4, pp. 193–202, 1989.

[8] M. Bendsoe, "Methods for optimization of structural topology, shape and material," 1995.

[9] O. Sigmund, "On the design of compliant mechanisms using topology optimization*," *Journal of Structural Mechanics*, vol. 25, no. 4, pp. 493–524, 1997.

[10] L. Yin and G. Ananthasuresh, "Topology optimization of compliant mechanisms with multiple materials using a peak function material interpolation scheme," *Structural and Multidisciplinary Optimization*, vol. 23, no. 1, pp. 49–62, 2001.

[11] R. Saxena and A. Saxena, "On honeycomb representation and sigmoid material assignment in optimal topology synthesis of compliant mechanisms," *Finite Elements in Analysis and Design*, vol. 43, no. 14, pp. 1082–1098, 2007.

[12] S. Rahmatalla and C. C. Swan, "Sparse monolithic compliant mechanisms using continuum structural topology optimization," *International Journal for Numerical Methods in Engineering*, vol. 62, no. 12, pp. 1579–1605, 2005.

[13] J. K. Guest, J. Prévost, and T. Belytschko, "Achieving minimum length scale in topology optimization using nodal design variables and projection functions," *International Journal for Numerical Methods in Engineering*, vol. 61, no. 2, pp. 238–254, 2004.

[14] J. K. Guest and J. H. Prévost, "A penalty function for enforcing maximum length scale criterion in topology optimization," in *11th AIAA/ISSMO multidisciplinary analysis and optimization conference proceedings (AIAA/ISSMO held in Portsmouth, VA), AIAA*, vol. 6938, 2006.

[15] M. Y. Wang, X. Wang, and D. Guo, "A level set method for structural topology optimization," *Computer methods in applied mechanics and engineering*, vol. 192, no. 1, pp. 227–246, 2003.

[16] M. Y. Wang, S. Chen, X. Wang, and Y. Mei, "Design of multimaterial compliant mechanisms using level-set methods," *Journal of Mechanical Design*, vol. 127, p. 941, 2005.

[17] M. Langelaar, "The use of convex uniform honeycomb tessellations in structural topology optimization," in *7th world congress on structural and multidisciplinary optimization, Seoul, South Korea, May*, pp. 21–25, 2007.

[18] C. Talischi, G. H. Paulino, and C. H. Le, "Honeycomb wachspress finite elements for structural topology optimization," *Structural and Multidisciplinary Optimization*, vol. 37, no. 6, pp. 569–583, 2009.

[19] A. Saxena, "Topology design with negative masks using gradient search," *Structural and Multidisciplinary Optimization*, vol. 44, no. 5, pp. 629–649, 2011.

[20] A. Saxena, R. Sauer, *et al.*, "Combined gradient-stochastic optimization with negative circular masks for large deformation topologies," *International Journal for Numerical Methods in Engineering*, vol. 93, no. 6, pp. 635–663, 2012.

[21] A. Saxena and G. Ananthasuresh, "On an optimal property of compliant topologies," *Structural and multidisciplinary optimization*, vol. 19, no. 1, pp. 36–49, 2000.

[22] A. Saxena and G. Ananthasuresh, "Topology synthesis of compliant mechanisms for nonlinear force-deflection and curved path specifications," *Journal of Mechanical Design*, vol. 123, no. 1, pp. 33–42, 2001.

[23] C. B. Pedersen, T. Buhl, and O. Sigmund, "Topology synthesis of large-displacement compliant mechanisms," *International Journal for numerical methods in engineering*, vol. 50, no. 12, pp. 2683–2705, 2001.

[24] A. Saxena, "Synthesis of compliant mechanisms for path generation using genetic algorithm," *Journal of Mechanical Design*, vol. 127, no. 4, pp. 745–752, 2005.

[25] I. Ullah and S. Kota, "Optimal synthesis of mechanisms for path generation using fourier descriptors and global search methods," *Journal of Mechanical Design*, vol. 119, no. 4, pp. 504–510, 1997.

[26] C. T. Zahn and R. Z. Roskies, "Fourier descriptors for plane closed curves," *Computers, IEEE Transactions on*, vol. 100, no. 3, pp. 269–281, 1972.

[27] A. K. Rai, A. Saxena, and N. D. Mankame, "Synthesis of path generating compliant mechanisms using initially curved frame elements," *Journal of Mechanical Design*, vol. 129, no. 10, pp. 1056–1063, 2007.

[28] A. K. Rai, A. Saxena, and N. D. Mankame, "Unified synthesis of compact planar path-generating linkages with rigid and deformable members," *Structural and Multidisciplinary Optimization*, vol. 41, no. 6, pp. 863–879, 2010.

[29] N. D. Mankame and G. Ananthasuresh, "Contact aided compliant mechanisms: concept and preliminaries," in *ASME 2002 International Design Engineering Technical Conferences and Computers and Information in Engineering Conference*, pp. 109–121, American Society of Mechanical Engineers, 2002.

[30] N. D. Mankame and G. Ananthasuresh, "Topology optimization for synthesis of contact-aided compliant mechanisms using regularized contact modeling," *Computers & structures*, vol. 82, no. 15, pp. 1267–1290, 2004.

[31] B. N. Reddy, S. V. Naik, and A. Saxena, "Systematic synthesis of large displacement contact-aided monolithic compliant mechanisms," *Journal of Mechanical Design*, vol. 134, no. 1, p. 011007, 2012.

[32] A. Saxena, "A material-mask overlay strategy for continuum topology optimization of compliant mechanisms using honeycomb discretization," *Journal of Mechanical Design*, vol. 130, p. 082304, 2008.

[33] A. Saxena, "An adaptive material mask overlay method: modifications and investigations on binary, well connected robust compliant continua," *Journal of Mechanical Design*, vol. 133, p. 041004, 2011.

[34] R. Saxena and A. Saxena, "On honeycomb parameterization for topology optimization of compliant mechanisms," ASME, 2003.

[35] M. S. Floater, "Mean value coordinates," *Computer Aided Geometric Design*, vol. 20, no. 1, pp. 19–27, 2003.

[36] K. Hormann, "Barycentric coordinates for arbitrary polygons in the plane," *Tech. rep., Clausthal University of Technology*, 2004.

[37] N. Sukumar and E. Malsch, "Recent advances in the construction of polygonal finite element interpolants," *Archives of Computational Methods in Engineering*, vol. 13, no. 1, pp. 129–163, 2006.

[38] N. Sukumar and A. Tabarraei, "Conforming polygonal finite elements," *International Journal for Numerical Methods in Engineering*, vol. 61, no. 12, pp. 2045–2066, 2004.